Progress In Electromagnetics Research C, Vol. 18, 153–168, 2011

CIRCULAR SLOT ANTENNAS USING L-SHAPED PROBE FOR BROADBAND CIRCULAR POLARIZATION

R. Joseph, S. Nakao, and T. Fukusako

Kumamoto University
2-39-1 Kurokami, Kumamoto 860-8555, Japan

Abstract—Novel circularly polarized antennas with a circular radiating aperture for broadband characteristics are presented in this paper. The vertical and horizontal components of the L-shaped probe are separated and placed at the front and back side of the substrate. The antennas are excited by a microstrip line which is connected to the vertical component of the L-shaped probe and electromagnetically couples the signal to the horizontal component of the L-shaped probe. A novel concept of placing stub in the slot of a planar antenna, by observing the electric field vector behaviour in the slot, is proposed to enhance the axial ratio (AR) bandwidth by around 10%. Unidirectional patterns can be obtained by having a cylindrical cavity of height $\lambda_g/4$ behind the antenna and is effective when no stubs are placed in the slot. $A < 3\,\text{dB}$ AR bandwidth of 39.5% with cavity and 41.18% without cavity but with stub in the slot is obtained in simulation and the results well match with the measurement.

1. INTRODUCTION

Circularly polarized (CP) broadband antennas have been received much attention recently for applications in wireless communication because they do not only reduce the multipath effects but also allow flexible polarization orientation of the transmitter and receiver antennas [1–4]. A printed slot antenna design is a desirable solution if the antenna bandwidth has to be improved without increasing the antenna size and thickness [5–7]. They provide bidirectional radiation along with greater manufacturing tolerances compared to microstrip patch antennas and well suits for applications that require both left hand circular polarization (LHCP) and right hand circular polarization

Received 9 November 2010, Accepted 6 December 2010, Scheduled 13 December 2010
Corresponding author: Ronald Joseph (ronald@st.cs.kumamoto-u.ac.jp).

(RHCP) for transmission and reception. Since the polarization sense changes from RHCP to LHCP and vice versa when reflected, an antenna which could receive both senses is significant, when the antenna need to receive the reflected signal if the direct signal is obstructed. For applications with switchable RHCP and LHCP, an unavoidable mute occurs because a new synchronization to the digital data stream is needed after switching from one beam to the other. An antenna which could receive both CP senses could avoid this problem and is used, for example, in satellite digital radio systems [15] and for the reception of terrestrial signals and signals of geostationary satellites [16].

Unidirectional patterns are also required for security, efficiency and other considerations in addition to wideband operation, especially for telecommunications and radars [9]. Cavity backed antennas [9–12] that radiate unidirectional patterns are of special interest because they can be easily mounted on surfaces of, for example, high speed vehicles with applications of mobile communication and radar systems. The inverted microstrip-fed cavity backed antenna in [11] claimed to have a CP bandwidth of 15% with a gain of 8.7 dBic. A circularly polarized cavity backed single element antenna in [12] attained a bandwidth of 20% in return loss and 24% in AR.

This paper presents a wideband planar bidirectional antenna in Section 2 and unidirectional cavity backed antenna in Section 3 with circular slot and separated L-shaped probes. A novel concept of placing a stub in the slot to enhance the CP bandwidth is also proposed in this paper. The circular slot cavity backed antenna in Section 3 is designed based on the principle of circular waveguide, to obtain unidirectional pattern. Broadband CP of 39.5% with cavity and 41.18% without cavity but with stub in the slot is achieved with the present design, which is much higher than the bandwidth obtained in [12].

2. ANTENNA WITH CIRCULAR SLOT AND STUB

2.1. Structure and Design

The structure of the antenna is shown in Fig. 1. The antenna uses a 0.8-mm thick Arlon diclad 522 substrate with a permittivity (ϵ_r) of 2.5 and dielectric loss ($\tan\delta$) of 0.001. The substrate dimension is fixed as $L_x = 82\,\text{mm}$ and $L_z = 81\,\text{mm}$ which are at $0.96\lambda_0$ and $0.95\lambda_0$ respectively, where λ_0 is the wavelength at the centre frequency f_0 of 3.5 GHz. This frequency is selected applying for, for example, 3.5 GHz WiMAX [4], chip-less RFID reader systems that make use of lower UWB technique [8] and pulse RADARs.

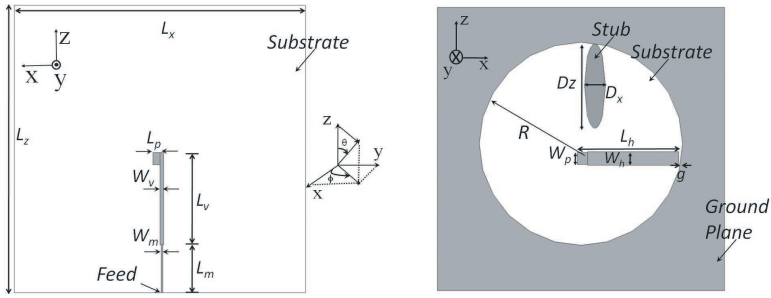

(a) Front View (b) Back View

Figure 1. Antenna with circular slot and stub.

The circular slot made at the centre of the ground plane has a radius (R) of 29 mm and designed to be around $0.34\lambda_0$ of the centre frequency. The horizontal and vertical components of the L-shaped probe are separated and placed at the front and backside of the substrate. The horizontal probe has a length (L_h) of 29 mm, which is designed at $0.34\lambda_0$. The vertical component of the L-shaped probe, designed at around $0.3\lambda_0$, is 26-mm long (L_v) and 1-mm wide (W_v). The vertical probe is extended to the edge of the substrate through a matching inductive microstrip feed line of 118 Ω with a width (W_m) of 0.4 mm and length (L_m) of 13.5 mm to match with the impedance of the 50 Ω coaxial cable.

The antenna is optimized using Ansoft HFSS 10.1 based on finite element method (FEM). The antenna is initially analysed without stub in the slot. In order to obtain broadband CP, capacitance in the structure need to be enhanced, for which a small gap (g) is created between the horizontal probe and ground plane and a small patch is placed at the end of the vertical probe.

The parameter g is studied in detail and its effect on S_{11} and AR are shown in Figs. 2(a) and 2(b) respectively. A shorted horizontal probe, when $g = 0$ mm, could not attain broadband S_{11} and unable to generate CP. The phase difference (PD) (Fig. 2(b)) between E_ϕ and E_θ is at 150° instead of 90° when $g = 0$ mm, and as g increases from 0.5 mm to 1.5 mm, the capacitance between the horizontal probe and ground plane reduces and PD becomes 75° from 90° at 3.5 GHz, which narrows down the AR characteristics. Even the S_{11} characteristics deteriorates with the increase in g because the impedance becomes more inductive but maintains a wide bandwidth. The antenna with a gap of 0.5 mm provided a bandwidth of 1.5 GHz at < -10 dB in S_{11} but only 0.7 GHz at < 3 dB in AR centred around 3.5 GHz.

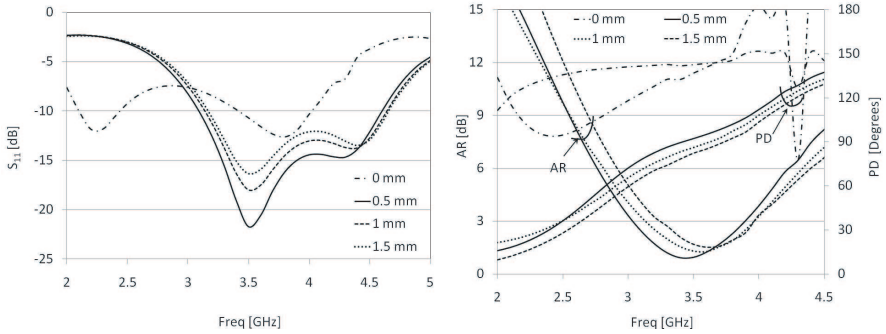

(a) (b)

Figure 2. Effect of gap g. (a) S_{11} Characteristics. (b) AR and PD Characteristics (in the direction $\phi = \theta = 90°$).

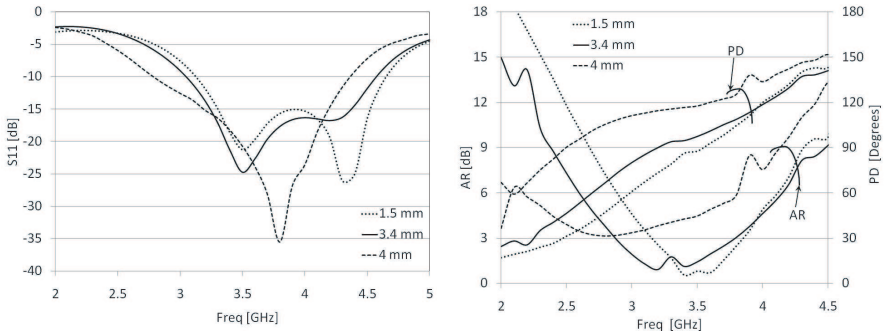

(a) (b)

Figure 3. Effect of patch width W_p. (a) S_{11} Characteristics. (b) AR and PD Characteristics (in the direction $\phi = \theta = 90°$).

In order to broaden the AR band, a 2-mm long patch (L_p) with a width of W_p is placed at the end of the vertical probe, which could enhance the the capacitance between the vertical and horizontal components of the L-shaped probe. The width of this patch equals the width of the overlapping region of the horizontal probe at the back side. The effect of W_p on S_{11} and AR characteristics for 1.5, 3.4 and 4 mm are shown in Fig. 3. The phase difference (PD) characteristics are included along with AR characteristics in Fig. 3(b).

The < -10 dB S_{11} bandwidth is around 1.2 GHz in all the cases but the resonance frequency varies because the impedance becomes capacitive with the increase in W_p. As W_p increases from 1.5 mm to 4 mm, the PD between E_ϕ and E_θ increases from 85° to 120° at 3.5 GHz. A width of 3.4 mm gives a PD of around 90° and has broader

AR characteristics. The width (W_h) of the remaining part of the horizontal probe is increased to 3.8 mm, which could also increase the capacitance in the antenna because of the capacitive gap at the end of the horizontal probe and the ground plane. The < 3 dB AR bandwidth is improved to 1 GHz when $W_p = 3.4$ mm and $W_h = 3.8$ mm but a more wider CP is needed for applications.

In order to further improve the CP bandwidth, the electric field vector behaviour at 3.5 GHz in the slot of the antenna is studied for one complete cycle and presented in Fig. 4. 0°, 120° and 240° represents the polarization phase of the electric field vector at respective instances. The current distribution vector, only in reg. 1, shows both counter clockwise (reg. 1́) and clockwise (reg. 1̋) rotations in the same region. So the electric fields in the neighbouring upper right region of the slot also shows the respective rotations. The current in reg. 2 shows complete clockwise rotation and so the electric field vector behaviour in the slot at the vicinity. When the phase is at 0°, the current in reg. 1́, reg. 2 and reg. 3 are directed to right, causes the electric field in the marked region in Fig. 4 to rotate left. When 120°, the currents in reg. 1́ and reg. 2 are directed to left but that in reg. 3 is directed to right, makes a downward polarization of the electric field vector. The electric field is directed to right when 240°, because the current in reg. 1́, reg. 2 and reg. 3 are directed to left. However, the electric field in the upper right region of the slot, in the vicinity of the horizontal

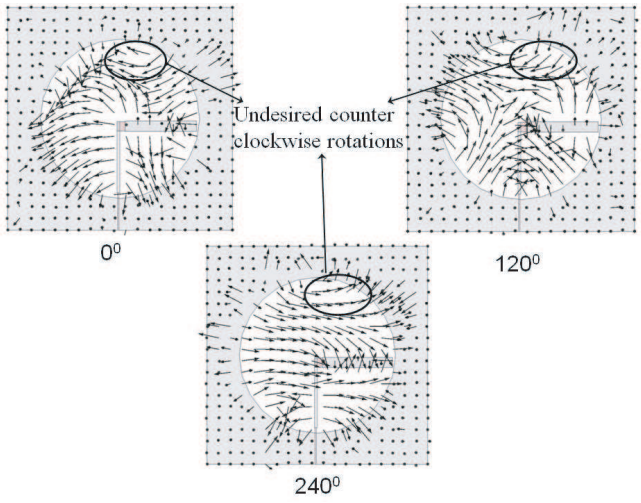

Figure 4. Electric field vector behaviour in the slot at 3.5 GHz.

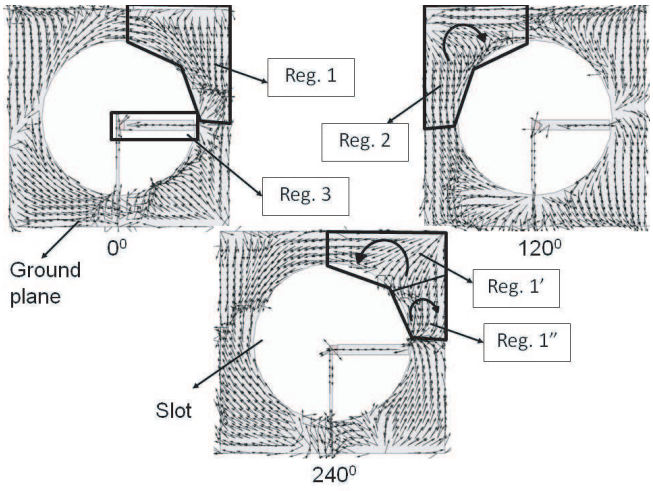

Figure 5. Current distribution at 3.5 GHz.

probe, is mainly affected by currents in reg. 1′′ and reg. 3, so the behaviour shows clockwise rotations and is different from the counter clockwise rotation generated by the marked region in Fig. 4. In order to eliminate the unwanted counter clockwise rotations developed at the marked region in Fig. 4, an oval shaped stub is attached to the ground plane at this specified region. Covering this region with a metal makes the electric field vector to be normal to the plane and avoids the generation of undesired counter clockwise rotations. In order for this, the shape and size of the stub and its position in the slot are to be carefully selected and optimized through parametric studies.

An oval shaped stub is selected since it could be easily attached to the circular shaped slot. This stub has a horizontal diameter (D_x) of 6.8 mm and vertical diameter (D_z) of 24 mm. The position of the stub is optimized at 4-mm offset from the centre, at the top end of the slot, in the positive x axis. This antenna is represented as $A1$ in the paper. The electric field vector behaviour in the slot is studied and the phase of the vector at 0°, 120° and 240° is shown in Fig. 6.

It could be observed from Fig. 6 that the vector rotation in the counter clockwise direction could be completely eliminated with the addition of the stub in the slot. The S_{11} and AR characteristics of this antenna $A1$ are included along with the measured results in Fig. 7. An improved wide < 3 dB AR bandwidth of around 1.5 GHz from 2.5 GHz to 4 GHz is achieved but the antenna resonates at a higher frequency of 4.7 GHz. The overlapped bandwidth between S_{11} and AR is also very narrow (3.3 GHz–4 GHz).

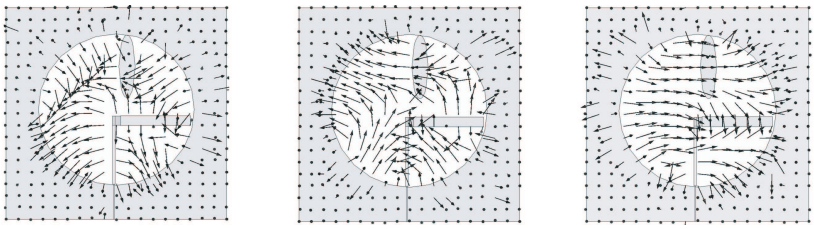

Figure 6. Electric field vector behaviour with stub in the slot at 3.5 GHz.

The slot is shifted in the positive z axis by 1.5 mm from the centre, with no variation in the x axis, together with the stub at the edge of the slot, to lower the resonance frequency to around 3.5 GHz and to achieve a good overlapped bandwidth, so that it will be useful for broadband applications. There are no variations in any other parameters of the antenna and even the capacitive gap (g) between the horizontal probe and ground plane is maintained. This antenna is called as $A2$ in the paper. The S_{11} and AR characteristics of this antenna $A2$ is also included with the measured results in Fig. 7. The S_{11} characteristics show slight deterioration in the characteristics because the input impedance becomes more inductive with the shift in the position of the slot but the resonance frequency could be lowered to 3.4 GHz. The AR bandwidth slightly narrows down to 1.4 GHz (2.7 GHz–4.1 GHz) because the amplitude of E_ϕ becomes more than the value of E_θ and also the phase difference between these two linear components becomes slightly more than 90°.

2.2. Experimental Results

The antenna ($A2$) with a stub in the slot and the slot position shifted by 1.5 mm in the positive z axis is fabricated on an Arlon diclad 522 substrate. The S_{11} and AR characteristics are presented in Figs. 7(a) and 7(b) respectively. The S_{11} characteristics show an improved bandwidth of 48.95% (2.7 GHz–4.45 GHz) in measurement at < -10 dB compared to that of 42.17% (2.9 GHz–4.45 GHz) at < -9 dB in simulation. The simulated AR characteristics at $\phi = \theta = 90°$, where ϕ and θ are the angle with respect to x and z axis respectively, show a < 3 dB bandwidth of 41.18% (2.7 GHz–4.1 GHz). The measured characteristics show a bandwidth of 44.78% from 2.6 GHz to 4.1 GHz. The small difference in the results may be due to fabrication tolerance because of the additional resistance and capacitance ensued during

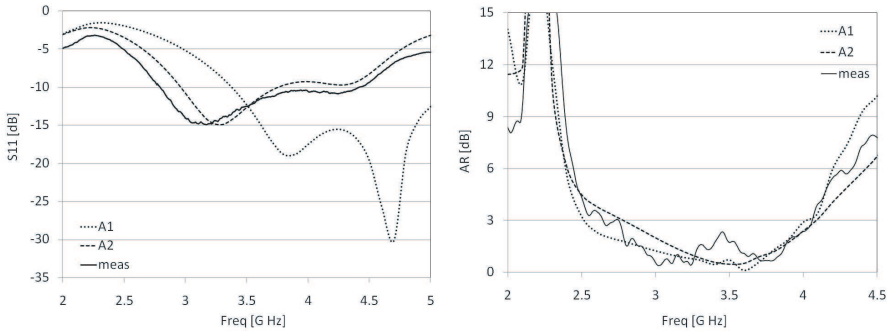

(a) (b)

Figure 7. Characteristics of the antenna. (a) S_{11} Characteristics. (b) AR Characteristics (in the direction $\phi = \theta = 90°$).

fabrication. The antenna has a good overlapped bandwidth of 41.18% from 2.7 GHz to 4.1 GHz.

The antenna generates bidirectional radiation pattern, simultaneous LHCP and RHCP, since it is a slot antenna. The simulated and measured radiation pattern characteristics of the antenna in x-y and y-z planes for frequencies 3 GHz, 3.5 GHz and 4 GHz are shown in Fig. 8. The frequencies in the AR band show good cross polarization discrimination (XPD) of more than 15 dB in simulation and 20 dB in measurement in a wide azimuth range from 30° to 120° at 3 and 3.5 GHz. A front to back (FB) ratio of more than 18 dB is achieved in both cases. The radiation pattern for 4 GHz show high cross polarization because the AR at this point is at 3 dB. The radiation pattern in y-z plane also shows very good agreement with the measured results. A XPD of more than 15 dB is achieved along with a FB ratio of more than 18 dB for 3 GHz. A XPD of around 15 dB is achieved in the range of 30° to 90° with a FB ratio of 28 dB at 3.5 GHz and more than 10 dB in XPD from 30° to 90° with a FB ratio of 20 dB at 4 GHz.

The measured and simulated gain characteristics of the antenna shown in Fig. 9 are well matched and a maximum gain of 5 dBic is obtained in a wide band.

3. CAVITY-BACKED ANTENNA

3.1. Structure and Design

As mentioned in Section 1, unidirectional patterns are required for security and efficiency in addition to wideband operation, especially

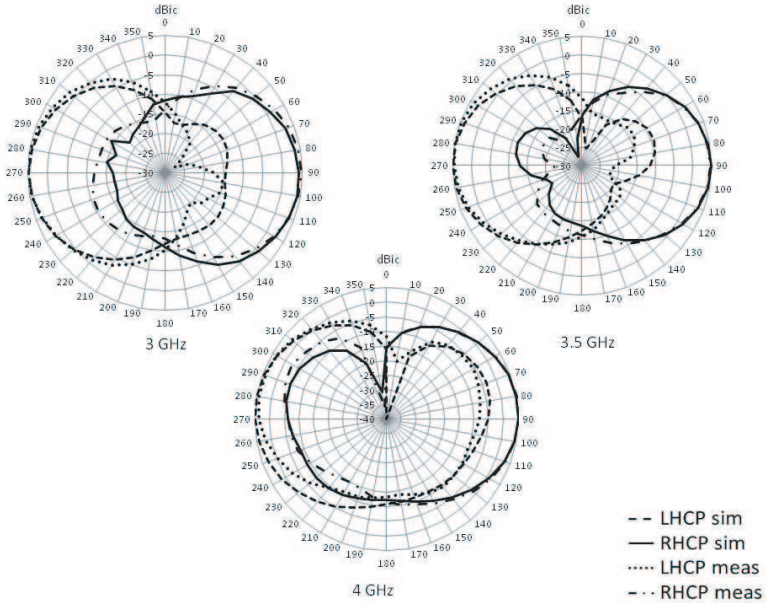

(a) *x*-*y* Plane

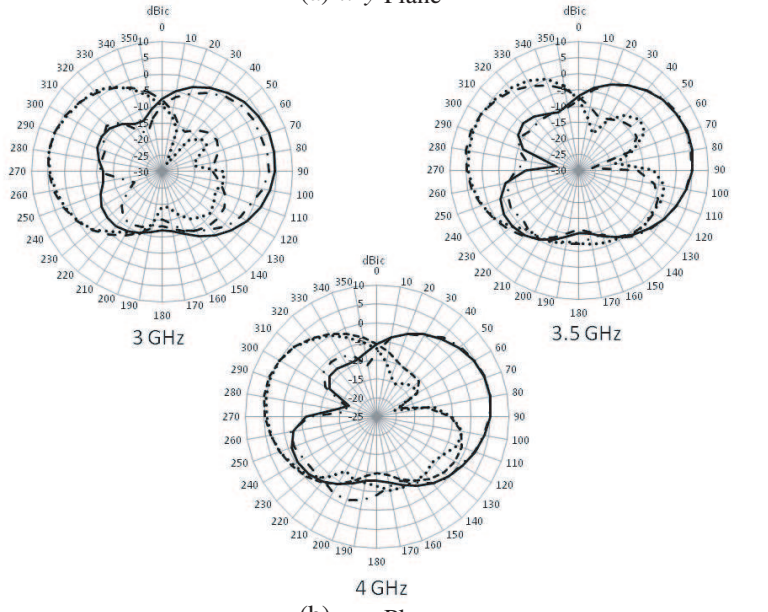

(b) *y*-*z* Plane

Figure 8. Radiation pattern.

for telecommunications and radar [9]. By having a reflector or a closed cavity at the back of the antenna, unidirectional patterns can be obtained. So the antenna explained in Section 2 is modified with a closed backed cavity and is shown in Fig. 10. Unlike other cavity backed antennas [11, 12], the cavity of this antenna has the same radius of the slot, without having any surrounding ground plane or substrate.

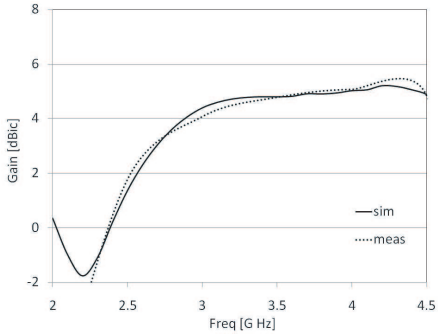

Figure 9. Gain characteristics.

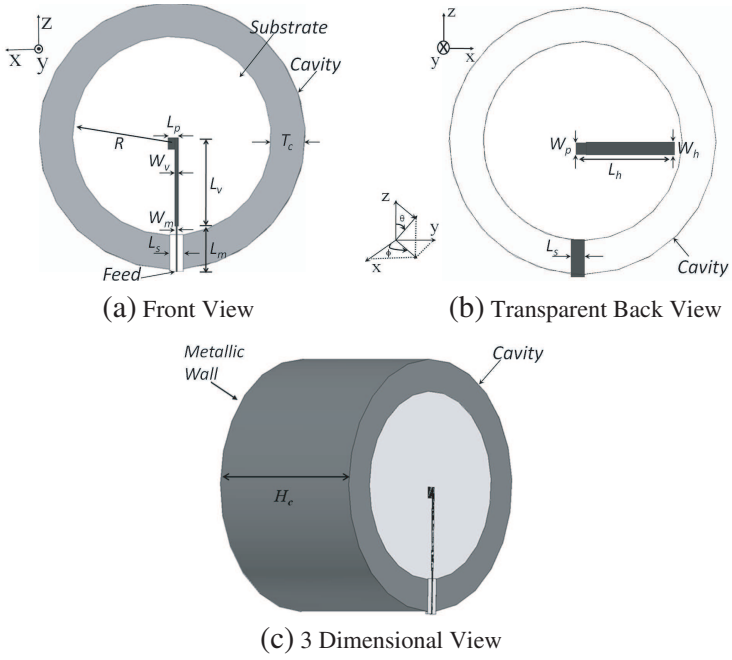

Figure 10. Cavity backed antenna.

The circular cavity is designed based on the principle of circular waveguide as explained in [13]. The dominant mode in circular waveguide, TE_{11}, with a radius a, has a cut off frequency designed by the formula

$$f_{TE_{11}} = \frac{P'_{11}}{2\pi a\sqrt{\mu_o\epsilon_o}} = 3.03\,\text{GHz}$$

The next higher order mode, TM_{01}, has a cut off frequency of

$$f_{TM_{01}} = \frac{P_{01}}{2\pi a\sqrt{\mu_o\epsilon_o}} = 3.9\,\text{GHz}$$

where P'_{11} and P_{01} are the mth root of bessel function J'_1 and J_0, so that $J'_1(P'_{11})$ and $J_0(P_{01})$ are zero. ϵ_o and μ_o are the permittivity and permeability in the free space respectively. P'_{11} and P_{01} has values 1.84 and 2.405 respectively for TE_{11} and TM_{01} modes. The centre frequency of operation is designed to be at 3.5 GHz, at the middle of the two frequencies $f_{TE_{11}}$ and $f_{TM_{01}}$. The height of the cavity (H_c) is fixed to be at 42 mm, which is at $\lambda_g/4$, where λ_g is the guided wavelength and is designed by the formula

$$\lambda_g = \frac{\lambda}{\sqrt{1-(\frac{f_c}{f})^2}}$$

where f and λ are the frequency and corresponding wavelength in free space and f_c is the frequency at the dominant mode.

Initially the antenna is simulated with a cavity wall thickness of 0.3 mm. The stub in the slot is removed and the the electric field vector behaviour in the slot of the antenna at 0°, 120° and 240°, which represents the polarization phase of the electric field vector at the respective instances, at 3.5 GHz is shown in Fig. 11. It is observed that the electric field vectors in the slot completely rotate in the clockwise direction. The radiated signal from the antenna to

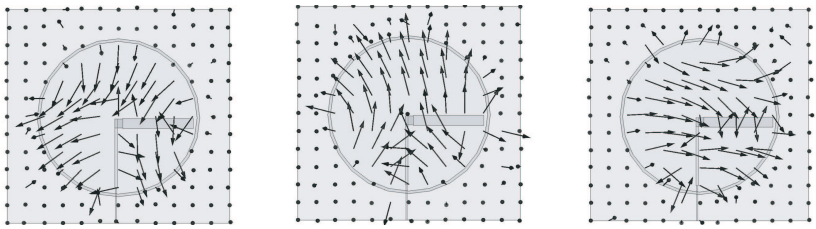

Figure 11. Electric field vector behaviour in the slot of cavity backed antenna at 3.5 GHz.

the closed cavity wall is LHCP and the reflected signal from this wall towards the antenna changes the polarization to RHCP. This RHCP signal incidents on the antenna and leads to total clockwise rotation in the slot and reduction of cross polarization. If a stub is placed in the slot, the vector behaviour will be disturbed and will result in the deterioration of CP. Comparing the electric field vector behaviours in the slot in Fig. 6 and Fig. 11, it could be noticed that the backed cavity also has the same effect of placing stub in the slot, which makes the electric field vectors in the slot to rotate in the clockwise direction. So, placing stub in the slot is effective only in planar structures without a backed-cavity.

Once the cavity is backed, the field is confined in the cavity. So the portion of the antenna outside the slot, i.e., the substrate and ground plane, except the region just below the micrstrip feed line, is removed and observed that this does not affect the antenna characteristics. The resonance frequency is remained at 3.5 GHz with an S_{11} bandwidth of around 1.3 GHz (2.9 GHz–4.2 GHz) and AR bandwidth of around 1.2 GHz (2.9 GHz–4.1 GHz).

The substrate and the ground plane beneath the feeding microstrip line has a width of L_s. This width, L_s, can be as small as 4 mm, but smaller widths deteriorates the S_{11} characteristics since the microstrip feed line will be at close proximity with the cavity wall.

Even the thickness of the cavity wall (T_c) has no effect on the antenna characteristics. This can be as thin as 0.1 mm but a thicker wall of 10 mm is preferred because it can be precisely fabricated and will not be easily mangled.

3.2. Experimental Results

The antenna is fabricated with a cavity made of aluminium and the simulated and experimental results of S_{11} and AR are presented in Fig. 12. An S_{11} bandwidth of 36.16% (2.9 GHz–4.18 GHz) at < -10 dB

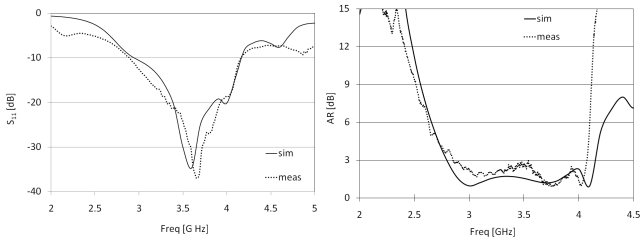

(a) (b)

Figure 12. Characteristics of the cavity-backed antenna. (a) S_{11} Characteristics. (b) AR Characteristics (in the direction $\phi = \theta = 90°$).

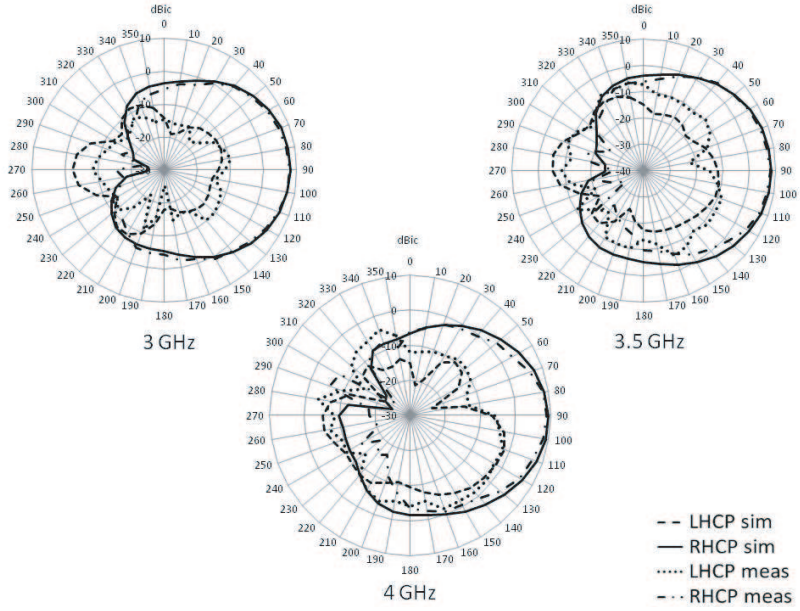

(a) x-y Plane

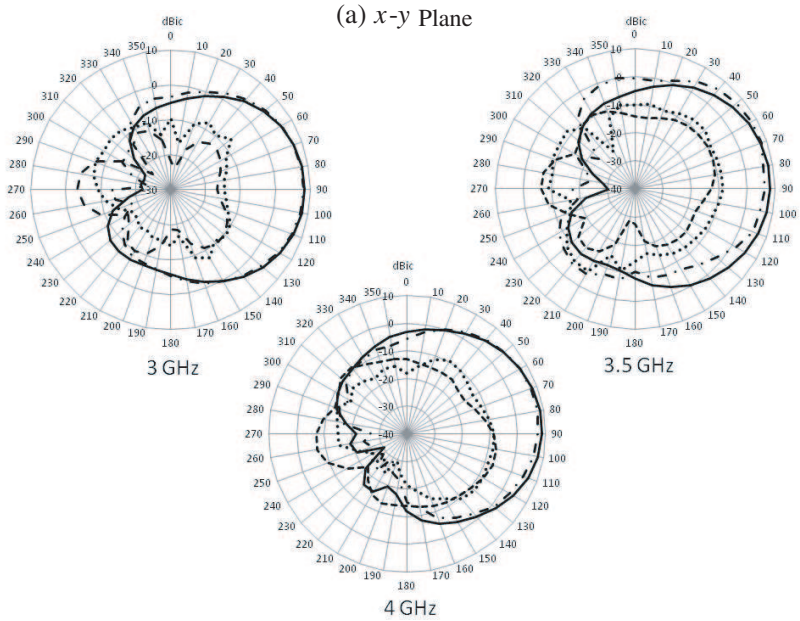

(b) y-z Plane

Figure 13. Radiation pattern.

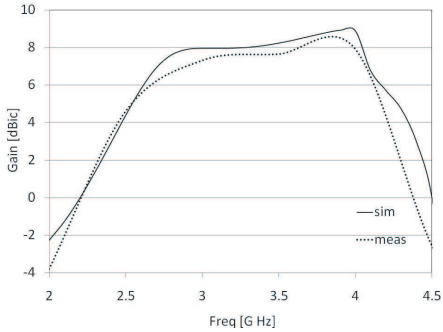

Figure 14. Gain characteristics.

and an AR bandwidth of 39.5% (2.78 GHz–4.15 GHz) at < 3 dB is obtained in simulation. The measured S_{11} characteristics well comply with the simulated results with a bandwidth of 37.16% (2.87 GHz–4.18 GHz). Even the measured AR characteristics are well matched with the simulation with a bandwidth of 36.3% (2.84 GHz–4.1 GHz).

The radiation pattern characteristics of the antenna in the x-y and y-z plane are presented in Fig. 13. The radiation pattern is unidirectional with a XPD of more than 20 dB in a wide azimuth range from 30° to 120° for 3 GHz and 3.5 GHz and from 0° to 100° for 4 GHz in x-y plane. The FB ratio is more than 35 dB in all the cases. The radiation pattern in y-z plane also shows good agreement between the measured and simulated results. A XPD of more than 15 dB is achieved in the entire azimuth range for 3 GHz and 3.5 GHz and from 20° to 110° in the case of 4 GHz. Also a FB ratio of more than 30 dB is achieved in all the three cases.

The simulated and measured gain characteristics of the antenna are presented in Fig. 14. The results show similar characteristics with a maximum gain of 9 dBic in simulation and 8.8 dBic in measurement. The gain remains almost constant in the desired operating band from 2.7 GHz to 4.1 GHz.

4. CONCLUSION

Broadband circularly polarized antennas with circular slot and separated L-probes are presented in this paper. Installation of an oval stub in the slot of a planar antenna, by observing the electric field vector behaviour, is proposed to eliminate the undesired electric field rotations and enhance the AR bandwidth. A closed backed cavity at the slot to obtain unidirectional broadband CP is effective only

when the antenna does not have stub in the slot. Electric field vector rotations in the clockwise direction can be obtained either by having a cavity or by placing stub in the slot. The planar antenna with stub in the slot could achieve a measured < -10 dB S_{11} bandwidth of 48.95% and < 3 dB AR bandwidth of 44.78%. A < -10 dB S_{11} bandwidth of 37.16%, < 3 dB AR bandwidth of 36.3% and a XPD of more than 20 dB on a wide azimuth range is achieved in measurement along with a maximum gain of 8.8 dBic, when the circular slot antenna is backed by a cavity. The bandwidth is slightly narrowed since the cavity limits the propagation of higher order modes.

REFERENCES

1. Chen, H. M., Y. K. Wang, Y. F. Lin, C. Y. Lin, and S. C. Pan, "Microstrip fed circularly polarized square ring patch antenna for GPS application," *IEEE Trans. Antennas Propag.*, Vol. 57, No. 4, 1264–1267, Apr. 2009.
2. Fukusako, T., K. Okuhata, K. Yanagawa, and N. Mita, "Generation of circular polarization using rectangular waveguide with L-type probe," *IEICE Trans. Commun.*, Vol. e86-B, 7, Jul. 2003.
3. Yang, S. S., K. F. Lee, A. A. Kishk, and K. M. Luk, "Design and study of wideband single feed circularly polarized microstrip antennas," *Progress In Electromagnetics Research*, Vol. 80, 45–61, 2008.
4. Masa-Campos, J. L. and F. Gonzalez-Fernandez, "Dual linear/circular polarized planar antenna with low profile double layer polarizer of 45° tilted metallic strips for WiMAX applications," *Progress In Electromagnetics Research*, Vol. 98, 221–231, 2009.
5. Tseng, L. Y. and T. Y. Han, "Microstrip fed circular slot antenna for circular polarization," *Microw. Opt. Technol. Lett.*, Vol. 50, No. 4, 1056–1058, Apr. 2008.
6. Chen, H. D, "Broadband CPW fed square slot antennas with wideband tuning stub," *IEEE Trans. on Antennas Propag.*, Vol. 51, No. 8, 1982–1986, Aug. 2003.
7. Jiao, J. J., G. Zhao, F. S. Zhang, H.-W. Yuan, and Y. C. Jiao, "A broadband CPW-fed T-shape slot antenna," *Progress In Electromagnetics Research*, Vol. 76, 237–242, 2007.
8. Preradovic, S., I. Balbin, N. C. Karmakar, and G. Swiegers, "A novel chipless RFID system based on planar multiresonators for barcode replacement," *2008 IEEE International Conference on RFID*, 289–296, Apr. 2008.

9. Qu, S. W., C. H. Chan, and Q. Xue, "Ultrawideband composite cavity backed folded sectoral bowtie antenna with stable pattern and high gain," *IEEE Trans. Antennas Propag.*, Vol. 57, No. 8, 2478–2483, Aug. 2009.
10. Shi, S., K. Hirasawa, and Z. N. Chen, "Circularly polarized rectangularly bent slot antenna backed by a rectangular cavity," *IEEE Trans. Antennas Propag.*, Vol. 49, No. 11, 1517–1524, Nov. 2001.
11. Li, Q. and Z. Shen, "An inverted microstrip fed cavity backed slot antenna for circular polarization," *IEEE Antennas and wireless Propag. Lett.*, Vol. 1, 190–192, 2002.
12. Hung, K. F. and Y. C. Lin, "Novel broadband circularly polarized cavity backed aperture antenna with travelling wave excitation," *IEEE Trans. Antennas Propag.*, Vol. 58, No. 1, 35–42, Jan. 2010.
13. Pozar, D. M., *Microrwave Engineering*, John Wiley and Sons, Inc., 2004.
14. Balanis, C. A., *Antenna Theory Analysis and Design*, John Wiley and Sons, Inc., 2006.
15. Saala, G., J. Hopf, and S. Lindenmeier, "Small satellite car antenna for simultaneous reception of LHCP and RHCP signals," *Third European Conference on Antennas Propag., EuCap 2009*, 2698–2700, Mar. 2009.
16. Saala, G., D. Muller, J. Hopf, and S. Lindenmeier, "Antenna with optimized pattern for simultaneous reception of terrestrial signals and signals of geostationary satellites," *Advances in Radio Science*, Vol. 8, 37–42, 2010.